Droplet Deformation and Structure Formation in Two-Phase Polymer/Polymer/Toluene Mixtures in an Electric Field

Kang Xi[1] and Sonja Krause*

Department of Chemistry and Polymer Science and Engineering Program, Rensselaer Polytechnic Institute, Troy, New York 12180-3590

Received November 10, 1997; Revised Manuscript Received March 9, 1998

ABSTRACT: Droplet deformation and the development of the final morphology after solvent evaporation were studied in two-phase ternary polymer/polymer/solvent mixtures in an electric field. The polymer mixtures used included polystyrene (PS) with such other polymers as poly(vinyl acetate) (PVA), poly(methyl methacrylate) (PMMA), or polybutadiene (PB) in toluene as a solvent. In a dc field, the dispersed phases were distorted into ellipsoids with their major axes either parallel (prolate ellipsoids) or perpendicular (oblate ellipsoids) to the field direction, and/or they aligned in the field direction to form pearl chains. Droplets of the dispersed phases sometimes coalesced to form columns either parallel or perpendicular to the electric field direction. Sometimes the droplets or columns broke up into smaller droplets in the dc field. The final morphology usually contained spheres or prolate or oblate ellipsoids either randomly distributed in the matrix or in the form of pearl chains or columns. It was found that the conductivity ratio between the dispersed and continuous phases is extremely important in structure formation in these nonconducting systems.

Introduction

The mechanical, chemical, electrical, and other properties of multicomponent and multiphase polymer systems are largely determined by their phase morphology and the nature of the interface between these phases. Therefore, control of morphology is the key to controlling the properties of such systems. Anisotropic morphologies, when they occur, are expected to result in anisotropic mechanical, electrical, and optical properties in polymer blends. Recently, it has been demonstrated[2−9] that electric fields can be used to control the orientation of the dispersed phase in polymer blends. This has opened a new option for the modulation of polymer blend morphology. Electric fields have also been used to make oriented structures in other polymer systems including one-[10,11] and two-phase[12,13] polymer solutions, block copolymer melts,[14−17] homopolymer/block copolymer mixtures,[18] and polymer/ceramic composites.[19,20]

Morphology development in polymer mixtures containing two immiscible homopolymers dissolved in a mutual solvent in the presence of a dc electric field during solvent evaporation was first investigated by Venugopal et al.[3−5] The polymer mixtures used included polystyrene (PS) with such other polymers as poly(ethylene oxide) (PEO), poly(methyl methacrylate) (PMMA), poly(vinyl acetate) (PVA), polybutadiene (PB), and poly(vinyl chloride) (PVC) in toluene or cyclohexanone as a solvent. They showed that when the dielectric constants of the dispersed phase (ϵ_d) and the matrix (ϵ_m) were about the same, namely, in the PS/PB/toluene system, there was no apparent droplet deformation. However, when the dispersed phase had a larger dielectric constant than the matrix in these ternary polymer mixtures, the droplets could be distorted into prolate ellipsoids with major axes in the field direction and/or formed pearl chains and columns in the field direction. In one case in which the dispersed phase (the PS-rich phase) had a smaller dielectric constant than the matrix (the PMMA-rich phase), using a 10/90 (w/w) PS/PMMA mixture in toluene, the PS-rich droplets appeared to be distorted into oblate ellipsoids with their major axes perpendicular to the field direction.

Observations of droplet elongation (to prolate ellipsoids) in the electric field direction can be explained by the pure dielectric theory of Garton and Krasucki.[21] This theory takes into account the effect of dielectric constant mismatch between the two phases, the interfacial tension between the phases, and the size of the droplets. It predicts that droplets are always distorted into prolate ellipsoids no matter whether the dispersed phase has a higher or lower dielectric constant than the matrix. Neither the observation of droplet elongation perpendicular to the electric field into oblate ellipsoids in the one case mentioned above nor the exact magnitude of the droplet elongations observed in the other cases could be explained by the Garton and Krasucki[21] theory. Only a leaky dielectric theory, as published by Torza et al.,[22] can predict the existence of droplet deformations both parallel and perpendicular to the electric field. In a leaky dielectric theory, the conductivity and viscosity mismatch between the two phases is taken into account along with all the parameters considered in the purely dielectric theory.

In the present work, we have used PS, PVA, PMMA, and PB in various three-component mixtures that always included toluene and PS as two of the components to study droplet deformation and structure formation in an electric field during solvent evaporation more thoroughly and to discover which parameters were the most important. It was shown that the conductivity mismatch between the two phases is extremely important in morphology formation in an electric field even in these systems which are essentially nonconducting; the absolute conductivity values of the coexisting phases in these mixtures were extremely low (on the order of 10^{-11}−10^{-12} S/m).

Experimental Section

Materials. Table 1 lists the molecular weights of all the polymers used in this work. These polymers were used as

S0024-9297(97)01650-1 CCC: $15.00
Published on Web 05/19/1998

Table 1. Molecular Weight Data of the Polymers Used

polymer	abbreviation	supplier	$M_w \times 10^{-5}$	M_w/M_n
styrene	PS	*a*	2.0	3.0
methyl methacrylate	PMMA	*b*	0.9	2.3
vinyl acetate	PVA	*c*	1.0	3.1
butadiene	PB	*a*	16.0	2.3

[a] Dow Chemical Co., Midland, MI. [b] Aldrich Chemical Co., Inc., Milwaukee, WI. [c] Scientific Polymer Products, Inc., Ontario, NY.

received, and HPLC toluene (Aldrich Chemical Co., Milwaukee, WI) was used as the solvent. The molecular weights of the polymers were determined as explained below. Lithium triflate (LiT) (Aldrich Chemical Co.) and ruthenium tetroxide (RuO_4) (5% by weight in an aqueous solution) (Polysciences, Inc., Warrington, PA) were also used in this work.

Preparation of Polymer Blend Samples. In the single-phase polymer mixtures that were prepared for method 1 experiments, the polymer content was usually 4% w/v (weight of polymer/volume of solution). The polymer portion of each mixture was prepared in various w/w ratios, shown, for example, as 1/9 PS/PVA.

To prepare coexisting phases for method 2 experiments, first two homopolymer solutions with relatively high polymer content were prepared, for example, 20% w/v. When these relatively concentrated polymer solutions were mixed, they immediately formed a turbid, phase-separated mixture which was then shaken vigorously for 5−10 min. The two phases were then allowed to separate from each other in a constant-temperature bath at 30 °C for about 4−8 weeks until two clear layers had formed. In some cases, LiT was added to PS/PMMA/toluene solutions to enhance the conductivity of the PMMA-rich phase since LiT can form a complex with PMMA.[23] The LiT was first added to a PMMA solution to make a saturated solution of LiT; then a PS solution was mixed with that PMMA solution, and the usual procedure to form coexisting phases was followed.

Some of the films of PS/PVA and PS/PB blends obtained after solvent evaporation in an electric field were stained with RuO_4. The polymer film was first placed on a glass slide; this slide, with the polymer film on its lower surface, was then placed at the top of a bottle containing several milliliters of a RuO_4/water solution. Staining time was about 0.5−1.5 h. In our cases, the darker phases were the PVA-rich and the PB-rich ones in the PS/PVA and PS/PB blends, respectively. Trent et al.[24] have reviewed the staining properties of RuO_4 for polymers.

Sample Characterization. Polymer molecular weights were determined by gel permeation chromatography (GPC) on a Viscotek model 100 instrument (Viscotek Corp., Houston, TX) with both viscosity and refractive index detectors, interfaced with an IBM-compatible computer. These measurements were carried out in tetrahydrofuran (THF) using two linear columns (American Polymer Standards Corp., Cleveland, OH; molecular weight range, $10^3-5 \times 10^6$). The universal calibration of molecular weights was done using PS standards (from Scientific Polymer Products, Inc., Ontario, NY).

Interfacial tensions between the coexisting phases were measured at 30 °C using a Krüss spinning drop interfacial tensiometer (Krüss USA, Ridge, NY). Such an instrument can be used to measure very small interfacial tensions.[25] The densities of the coexisting phases that were required to calculate the interfacial tensions were measured at 30 °C using a Parr DMA 48 densitometer (Anton Paar, Graz, Austria) which was able to provide four significant figures after the decimal point.

Dielectric constants of the coexisting phases were calculated from the ratio of the capacitance of each phase with respect to the capacitance of air as measured at 1 kHz at room temperature using a Solartron model 1260 impedance/gain-phase analyzer (Solartron Inc., Allentown, PA). The conductivities of the coexisting phases were calculated from the resistance values of the solutions. The resistances were measured at room temperature using a Keithely model 616 digital electrometer (Keithely Instruments, Inc., Cleveland, OH). These measurements were carried out in the laboratory of G. E. Wnek.

Viscosities of the coexisting phases were determined at 30 °C using a Brookfield model DV-II+ digital cone/plate viscometer (Brookfield Engineering Laboratories, Inc., Stoughton, MA) with a 0.5-mL cell. Spindle speeds of 1−100 rpm were used, giving shear rates in the range of 3.84−384 s^{-1}. The results showed that the viscosities of the demixed solutions were independent of shear rates in this range.

The compositions of the coexisting phases in the PS/PVA/toluene and PS/PMMA/toluene systems were determined as follows. (The procedure has been discussed in detail by Venugopal et al.[3]). Briefly, a small amount of one of the coexisting phases was removed using a syringe and weighed. The solvent was evaporated from that phase, and the residual polymer was weighed to give the weight percent of both polymers together in that phase. The ratio of the two polymers was then determined by ^1H NMR using a 200-MHz Varian VI-200 Fourier transform (FT) spectrometer. The solvent used was $CDCl_3$, and tetramethylsilane (TMS) was used as an internal reference.

Apparatus Used in Experiments under an Electric Field. Figure 1 shows a schematic diagram of the experimental setup. The experiments were carried out under a Leitz Laborlux 12 Pol S microscope with magnification 32× and 10× for the objective lens and the eyepiece, respectively. A glass window was used to cover the sample from the top to slow solvent evaporation as well as to keep the evaporated solvent away from the objective lens. A digital model XC-77 CCD camera (Hamamatsu Corp., Bridgewater, NJ) was connected to the eyepiece of the microscope. The images were taken, analyzed, and printed out using an IBM-compatible computer with Optimas Image Analysis 4.01 software (Optimas Corp., Bothell, WA).

The electrodes used were made by adhering copper (or aluminum) metal strips (about 1.3-mm thicknesses) onto a glass slide. The gap between the electrodes was adjusted to be around 2−3 mm. Both Hewlett-Packard 6515A (Hewlett-Packard Co., Wilmington, DE) and Trek model 610C (Trek, Inc., Medina, NY) high-voltage supplies/amplifiers were used to apply dc electric fields up to 10 kV. When ac fields were desired, a SRS model DS 335 synthesized function generator (Stanford Research Systems, Sunnyvale, CA) was used with the Trek model 610C amplifier to provide up to 7 kV ac.

Two methods, both at room temperature, were used to observe the effect of an electric field on our systems. In method 1, a small amount of a solution of a single-phase polymer blend was applied to the gap between the electrodes on the glass slide. Then the electric field was turned on while the solvent evaporated. Once most of the solvent had evaporated and the morphology was frozen, the electric field was turned off. In method 2, a small amount of one of the coexisting phases prepared earlier was placed on the glass slide between the electrodes. Droplets of the other coexisting phase were injected into this matrix using a 10-μL syringe. Then an electric field was applied to the sample.

Results and Discussion

Phase Diagrams and Phase Properties of the Polymer/Polymer/Toluene Mixtures. The experimentally obtained phase compositions and simulated binodals, spinodals, and tie lines of the PS/PVA/toluene and PS/PMMA/toluene systems are shown in Figures 2 and 3, respectively. These figures are drawn as if these systems were true three-component systems, which they are not, because each polymer is, by itself, a multicomponent system. Figures 2 and 3 are therefore pseudo-three-component phase diagrams; such diagrams are sufficient for the discussions in this work. Such systems have been discussed at length by Kurata[26] and Kamide.[27] The tie lines in Figures 2 and 3 indicate that the toluene content in the PS-rich phases was slightly

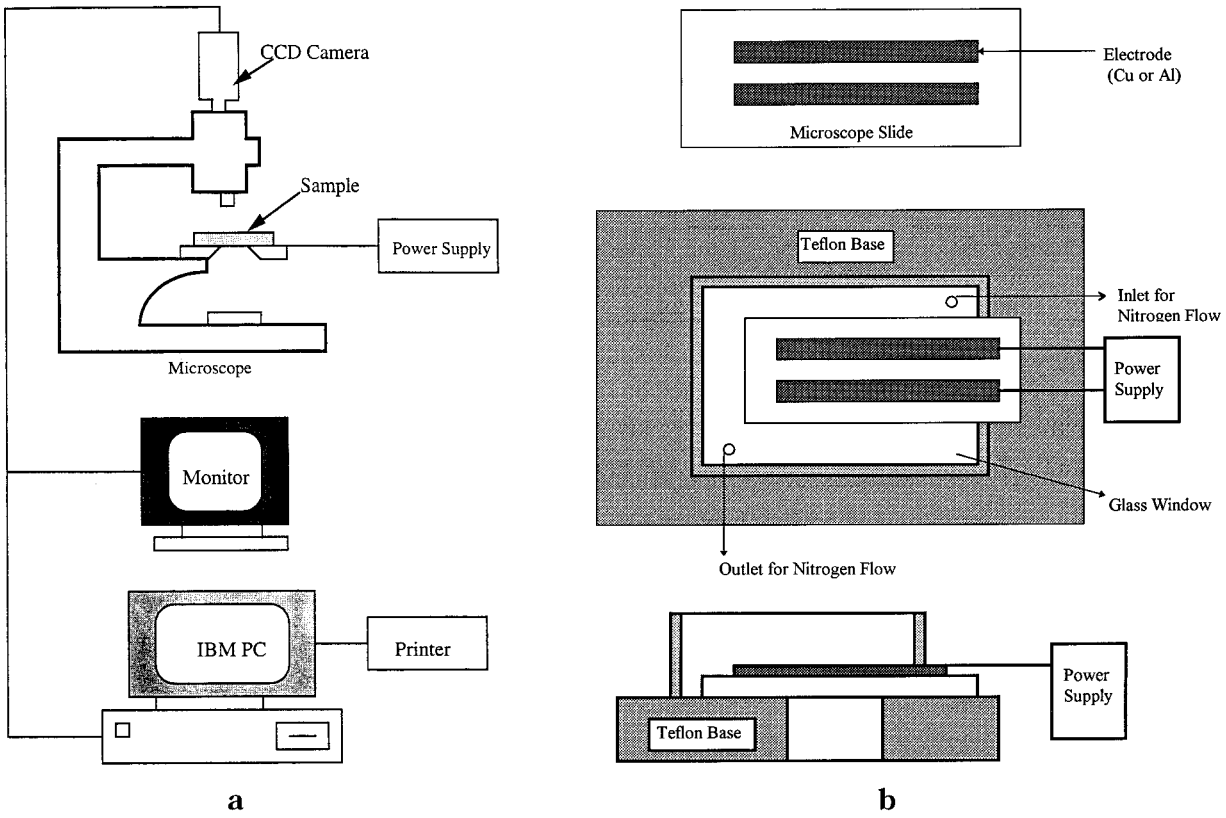

Figure 1. Experimental setup, including electrode design, for the study of the effect of an electric field on polymer blends during solvent evaporation.

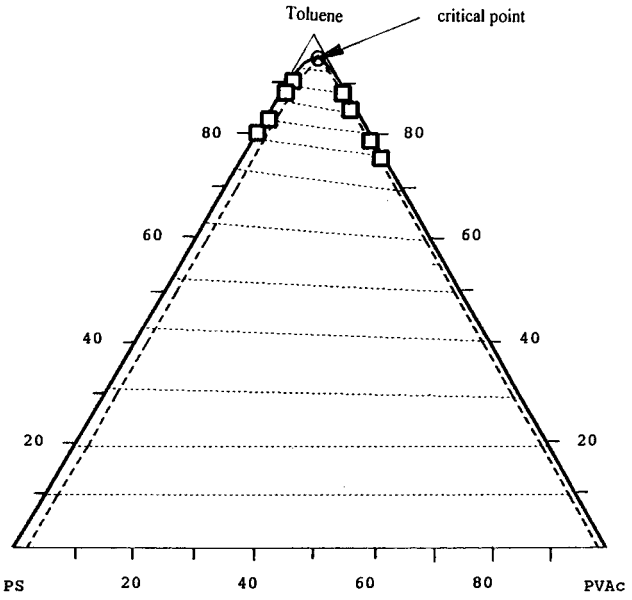

Figure 2. Pseudo-ternary phase diagram of the PS/PVA/toluene system at 30 °C. The numbers along the edges of the triangle refer to the volume percent of the appropriate component: —, simulated binodal curve; – –, simulated spinodal curve; ···, simulated tie line; □, experimental data.

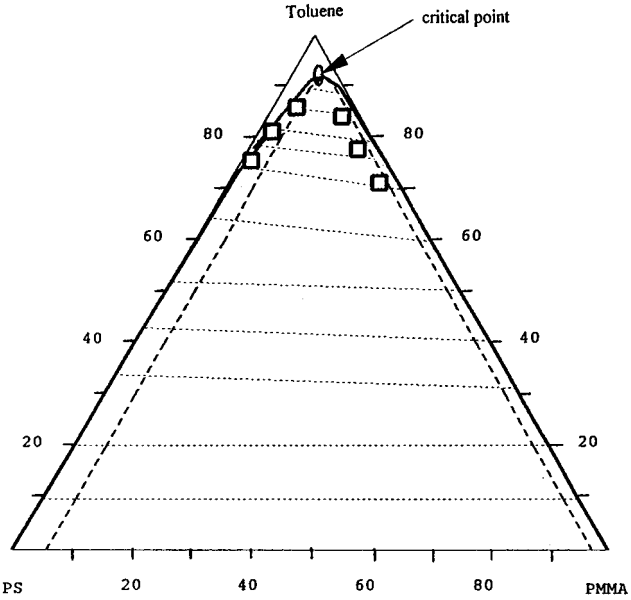

Figure 3. Pseudo-ternary phase diagram of the PS/PMMA/toluene system at 30 °C. The number along the edges of the triangles refer to the volume percent of the appropriate component: —, simulated binodal curve; – –, simulated spinodal curve; ···, simulated tie line; □, experimental data.

higher than that in the other phases in both systems. Thus, toluene was a better solvent for PS than for PVA and PMMA in these systems even though the M_w of PS was higher than those of PVA and PMMA (Table 1). One may note that the concentration of the minority component in any phase was always very low, since these high molecular weight polymers were very immiscible. The simulated spinodals and binodals of these systems at 30 °C, using the Flory–Huggins theory for a three-component system,[28] were calculated using Flory interaction parameters chosen from the literature[29] to give good agreement with the experimentally obtained tie lines. They were $\chi_{PS/toluene} = 0.40$ (literature values: 0.40–0.44), $\chi_{PVAc/toluene} = 0.47$ (literature values: 0.47–0.50), $\chi_{PMMA/toluene} = 0.47$ (literature values: 0.45–0.47), and $\chi_{PS/PMMA} = 0.01$ (literature values: 0.009–0.04). In the case of the PS–PVA interaction parameter, no literature value was found, but the calculated value for

Table 2. Electric Properties of Toluene and of the Coexisting Phases of the PS/PVA, PS/PMMA, and PS/PB Mixtures in Toluene at Room Temperature[a]

system	total polymer (wt %)	dielectric constant ϵ[b]	conductivity σ (S/m)[b]	ϵ_i/ϵ_a[c]	σ_i/σ_a[c]
HPLC toluene		2.38[d]	1.0×10^{-11}		
PS/PVA/toluene	10	2.45 (a)	1.3×10^{-11} (a)	1.15	14
		2.82 (b)	1.9×10^{-11} (b)		
	15	2.37 (a)	8.9×10^{-12} (a)	1.36	19
		3.22 (b)	1.7×10^{-10} (b)		
	20	2.37 (a)	6.3×10^{-12} (a)	1.38	28
		3.28 (b)	1.8×10^{-10} (b)		
	25	2.44 (a)	2.1×10^{-12} (a)	1.74	228
		4.24 (b)	4.8×10^{-10} (b)		
PS/PMMA/toluene	10	2.55 (a)	6.1×10^{-12} (a)	1.08	4.5
		2.76 (c)	2.7×10^{-11} (c)		
	20	2.56 (a)	5.9×10^{-12} (a)	1.13	5.4
		2.91 (c)	3.2×10^{-11} (c)		
	25	2.50 (a)	3.7×10^{-12} (a)	1.18	9.6
		3.11 (c)	3.6×10^{-11} (c)		
PS/PMMA/toluene (with added LiT Salt)	20	2.40 (a)	4.3×10^{-10} (a)	1.18	41
		2.84 (c)	1.8×10^{-8} (c)		
PS/PB/toluene	5	2.35 (a)	3.2×10^{-10} (a)	1.00	1.06
		2.36 (d)	3.4×10^{-8} (d)		

[a] Room temperature was in the range 25−30 °C. [b] (a) the PS-rich phase; (b) the PVA-rich phase; (c) the PMMA-rich phase; (d) the PB-rich phase. [c] Subscripts a and i refer to phases a and i, respectively. [d] Reference 30.

Table 3. Viscosity, Density, and Interfacial Tensions of the Coexisting Phases of the PS/PVA/Toluene, PS/PMMA/Toluene, and PS/PB/Toluene Mixtures at 30.0 °C

system	total polymer (wt %)	viscosity (cP)[a]	density (g cm^{-3})[a]	interfacial tension (N/m)
PS/PVA/toluene	10	13.1 (a)	0.8820 (a)	1.44×10^{-5}
		13.8 (b)	0.8930 (b)	
	15	30.4 (a)	0.8859 (a)	7.60×10^{-5}
		30.5 (b)	0.9061 (b)	
	20	65.5 (a)	0.8916 (a)	1.22×10^{-4}
		84.5 (b)	0.9207 (b)	
	25	136.8 (a)	0.9037 (a)	2.40×10^{-4}
		189.6 (b)	0.9395 (b)	
PS/PMMA/toluene	15	20.5 (a)	0.8895 (a)	3.80×10^{-6}
		17.0 (c)	0.9074 (c)	
	20	54.7 (a)	0.8916 (a)	3.15×10^{-5}
		55.0 (c)	0.9207 (c)	
	25	161.6 (a)	0.9044 (a)	9.08×10^{-5}
		187.7 (c)	0.9395 (c)	
PS/PB/toluene	5	10.8 (a)	0.8703 (a)	6.1×10^{-6}
		60.7 (d)	0.8614 (d)	

[a] (a) the PS-rich phase; (b) the PVA-rich phase; (c) the PMMA-rich phase; (d) the PB-rich phase.

$\chi_{PS/PVAc}$ at 30 °C was 0.02 using solubility parameters[29] $\delta_{PS} = 18.5$ MPa and $\delta_{PVAc} = 19.2$ MPa. The simulations were performed on a UNIX workstation using Maple software. The spinodal curve was solved analytically, and the binodal was calculated numerically. The general features of the phase diagram for the PS/PMMA/toluene system shown in Figure 3 agree well with those obtained by Venugopal et al.[4]

Tables 2 and 3 show some of the measured properties of the toluene and of the coexisting phases obtained in the PS/PVA/toluene, PS/PMMA/toluene, and PS/PB/toluene mixtures. Only one coexisting pair of phases was prepared in the PS/PB/toluene system because the viscosity of the PB-containing solutions was very high. This made it difficult for the PS/PB/toluene demixed solutions to reach equilibrium at high polymer content. The literature values for the homopolymer dielectric constants[30] at 25 °C for PS and PB are ∼2.4, those for PMMA and PVA are ∼3.5, and that for toluene[31] is 2.38, all rather close together. Table 2 shows that the dielectric constants of the PVA-rich and PMMA-rich phases were, as one might expect, slightly larger than those of the PS-rich phases. In the case of the PS/PB/toluene system, the dielectric constants of the two coexisting phases were very close to each other, again, as one might expect from the dielectric constant of the pure homopolymers in the solid state. The conductivities of the coexisting phases in all the mixtures were extremely low, comparable to that of the HPLC toluene used as the solvent. Since PS, PVA, PMMA, PB, and toluene are all usually considered to be nonconducting materials, these conductivities probably come from tiny amounts of ionic species which are possible impurities in these materials. Small amounts of ionic species may, however, be intrinsic to these materials, especially the solvent.[32] The conductivities of the PVA-rich and PMMA-rich phases were always higher than those of the PS-rich phases in the PS/PVA/toluene and PS/PMMA/toluene mixtures, respectively. Since PVA and PMMA have more polar side groups (therefore higher dielectric constants) than PS, this is not unexpected. One may also notice that the conductivities of the PS-rich phases in these mixtures were actually lower than that of the solvent alone. This shows that some of the ionic impurities present in the pure solvent must have migrated into the phase with the higher dielectric constant in each case. In the PS/PB/toluene mixture, both the conductivities and the dielectric constants of the two coexisting phases were very close to each other, the values of both being slightly higher in the PB-rich phase. The ratios of the dielectric constants and conductivities between the coexisting phases, also shown in Table 2, indicate that, although the dielectric constant ratios were close to 1, the conductivity ratios were not, except in the case of the PS/PB/toluene mixtures. The conductivity ratios in the PS/PMMA/toluene system were smaller than those in the PS/PVA/toluene system at the same polymer content, indicating that PMMA had less ability to associate with ionic species than PVA. One may also note that the ratios of conductivity and dielectric constant increased with increasing polymer content.

The viscosities, densities, and interfacial tensions of the coexisting phases of the PS/PVA/toluene, PS/PMMA/toluene, and PS/PB/toluene mixtures at 30.0 °C are listed in Table 3. As expected, the viscosities and the densities of the coexisting phases both increased with increasing polymer concentration. The interfacial tensions also increased with increasing polymer concentration, because, in the systems investigated, the critical points in the phase diagrams (Figures 2 and 3) were situated near the high solvent concentration portions of the phase diagrams. It is well-known that the interfacial tension between coexisting phases increases as the tie lines move farther away from the critical point; the interfacial tension must tend to zero at the critical point.

Observation of dc-Electric-Field-Induced Structures in Polymer Blends during Solvent Evaporation. In general, when using method 1, a certain amount of bulk fluid swirling motion was always observed during solvent evaporation when solvent content was relatively high, consistent with the observations of Venugopal et al.[4] The magnitude of the motion increased dramatically with increasing electric field

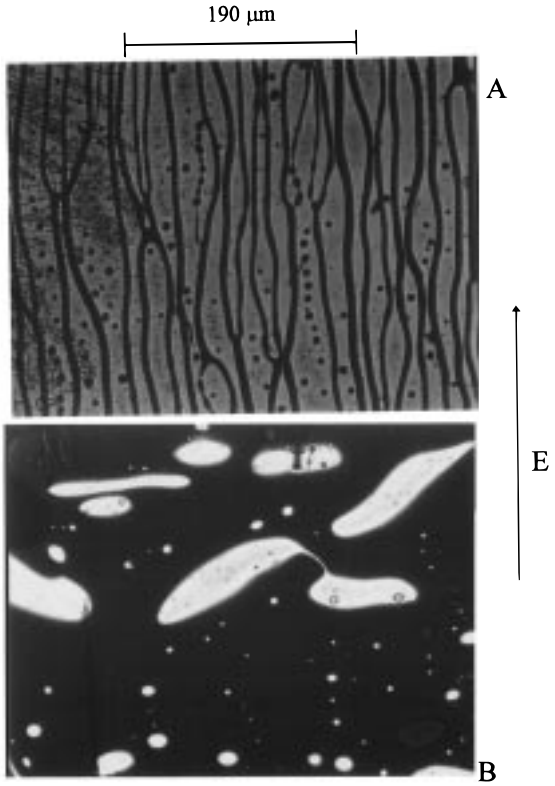

Figure 4. Final morphology of some PS/PVA blends prepared by solvent evaporation and stained with RuO_4. The darker phase is the PVA-rich phase. (A) 9/1 (w/w) PS/PVA at $E = 4$ kV/cm; (B) 1/9 (w/w) PS/PVA at $E = 7$ kV/cm.

strength. Due to this bulk fluid motion, no stable structures were obtained in the early stages of solvent evaporation. The motion decreased a great deal with decreasing solvent content due to an increase in solution viscosity, and stable structures were obtained in the relatively later stages of the evaporation. When most of the solvent had evaporated, the morphology (or structure) became the final morphology.

Figure 4 shows the stained final morphology of two PS/PVA blends made in a dc field; the darker phase is the PVA-rich phase. When the PVA-rich phase formed the dispersed phase, it was elongated in the field direction and formed some column-like structures (Figure 4A); when the PS-rich phase formed the dispersed phase, it was elongated more or less perpendicular to the field direction (Figure 4B). Figure 5 shows electric-field-induced structures in a particular PS/PVA/toluene blend containing equal weights of the two polymers during solvent evaporation at two different fields. At 2.3 kV/cm, the dispersed, presumably PVA-rich, phase existed as prolate ellipsoids aligned in the field direction to form pearl chains (Figure 5A). When the field was increased to 4.5 kV/cm, these ellipsoids in the pearl chains fused together, resulting in very long columns (Figure 5B) across the electrodes. The pearl chains (the PVA-rich phase) formed during solvent evaporation remained present until most of the solvent had evaporated when the electric field was relatively small.

Figure 6A shows the pearl chains formed during solvent evaporation in a blend of 1/9 (w/w) PS/PVA in toluene at $E = 9.7$ kV/cm. In this case, the dispersed phase, presumably the PS-rich phase, was elongated perpendicular to the field direction. This type of pearl chain, however, did not remain present for a long time during solvent evaporation since the droplets fused

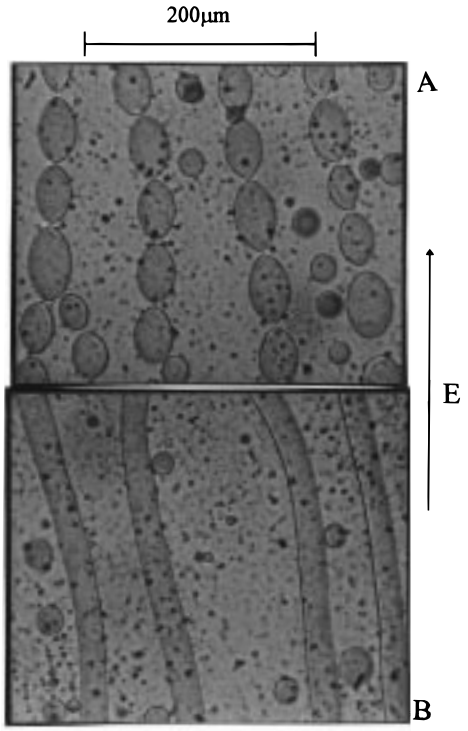

Figure 5. Electric-field-induced morphologies of 1/1 (w/w) PS/PVA in toluene during solvent evaporation: (A) at $E = 2.3$ kV/cm; (B) when the electric field was increased to $E = 4.5$ kV/cm.

quickly, probably due to the large contact areas between the droplets (see Figure 6B,C). The final morphology in this case usually consisted of prolate ellipsoid-like structures with large deformations perpendicular to the field direction (see also Figure 4B).

Figure 7 shows that droplet elongations both parallel and perpendicular to the field direction were also observed in the PS/PMMA/toluene system. One may note that the deformations were relatively small, especially for the smaller droplets which remained relatively spherical. No pearl chains and column structures were observed in PS/PMMA blends under a dc field (0−25 kV/cm), except after adding LiT salt to the mixtures (not shown).

In the PS/PB/toluene system, the observed droplet deformations were small even at a high field as shown in Figure 8. As mentioned above, Venugopal et al.[5] observed no droplet distortions at all in a somewhat lower electric field[33] using a similar mixture containing somewhat lower molecular weight polymers with different molecular weight distributions. The darker phase in this case is the PB-rich phase. One may note that the PS-rich droplets elongated either in the field direction or perpendicular to the field direction or remained relatively spherical in shape. This was also observed when method 2 was used, that is, after droplets of the PS-rich coexisting phase were injected into a matrix of the PB-rich coexisting phase (Figure 9). No pearl chain or columnar structures were observed in this system.

Breakup of deformed droplets was sometimes observed in the PS/PVA/toluene system during solvent evaporation as shown in Figures 10 and 11. Figure 10 shows a presumably PVA-rich droplet, elongated in the direction of the electric field, that has formed a neck near the center and is in the process of breaking up into two smaller drops. Figure 11A shows a presumably PS-

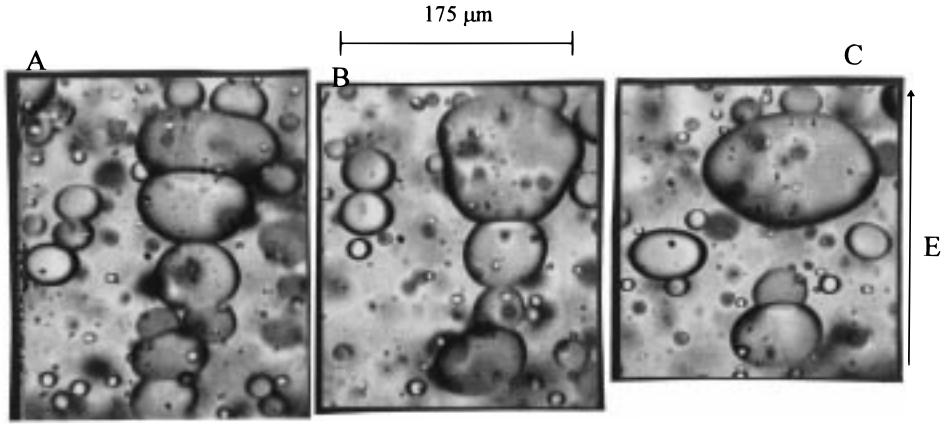

Figure 6. Process of fusion of pearl chains in a blend of 1/9 (w/w) PS/PVA in toluene at $E = 9.7$ kV/cm during solvent evaporation: (A) at t_0; (B) at $t_0 + 3$ s; (C) at $t_0 + 5$ s.

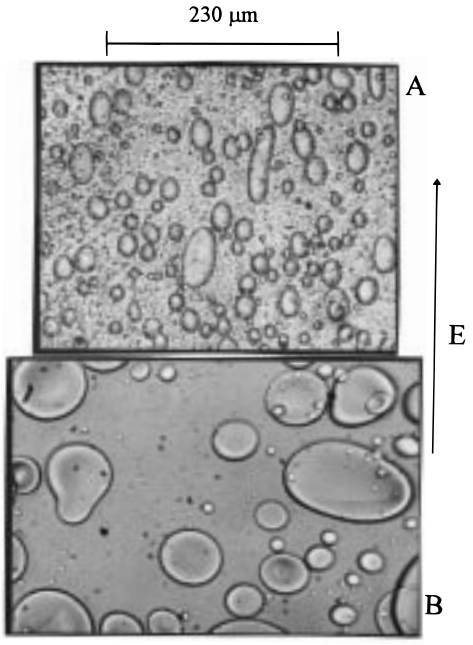

Figure 7. Final morphologies of PS/PMMA blends in toluene made in a dc field during solvent evaporation: (A) 3/1 (w/w) PS/PMMA at $E = 11$ kV/cm; (B) 1/9 (w/w) PS/PMMA at $E = 9.7$ kV/cm.

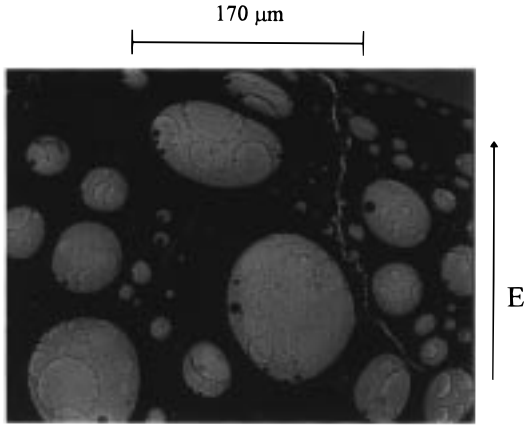

Figure 8. Final morphology (stained with RuO_4) of a blend of 1/5 (w/w) PS/PB made in a dc field of 12 kV/cm during solvent evaporation. The darker phase is the PB-rich phase.

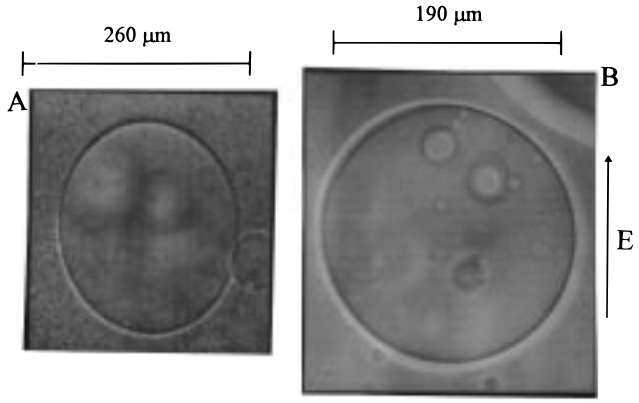

Figure 9. Deformation of droplets of the PS-rich phase injected into the matrix of the PB-rich phase at $E = 0.3$ kV/cm (using a 1/1/8 by weight PS/PB/toluene demixed solution): (A) a droplet elongated parallel to the field direction; (B) an undeformed droplet. Although some droplets were elongated perpendicular to the field direction, none of these is shown.

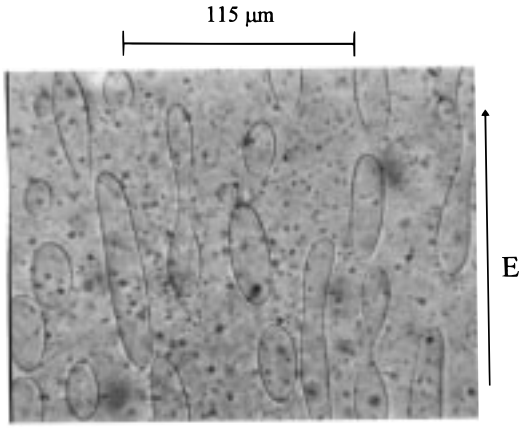

Figure 10. Breakup of some presumably PVA-rich droplets in a blend of 4/1 (w/w) PS/PVA in toluene at $E = 3$ kV/cm during solvent evaporation.

rich column, elongated in a direction perpendicular to the electric field, which has formed several necks and has partially broken up. Parts B and C of Figure 11 show an elongated PS-rich droplet in a PVA-rich matrix in the process of breaking up. It was found that when the axial ratio (the major axis vs the minor axis) was relatively small, the droplets were stable. However, once the axial ratio of a droplet exceeded 2, the droplets became unstable. When the droplets had become sufficiently elongated perpendicular to the field direction as in Figure 11, their shape changed constantly with time until they broke up. Long columns sometimes formed during the breakup process. Since the solution

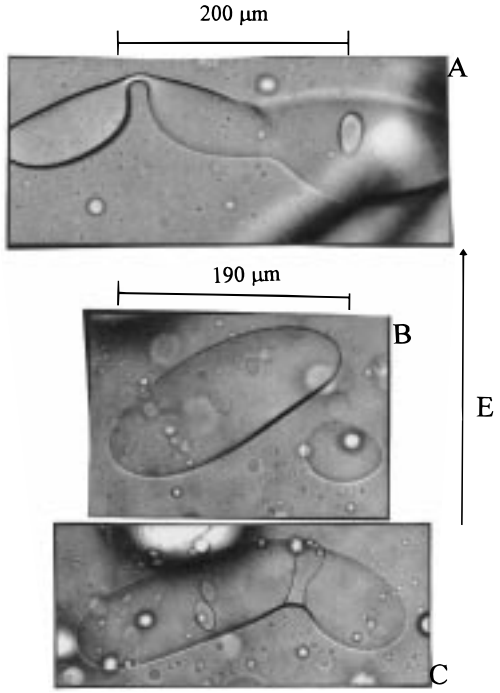

Figure 11. Breakup of presumably PS-rich columns and droplets in a PVA-rich matrix during solvent evaporation: (A) breakup of a column at $E = 8$ kV/cm, 1/9 PS/PVA in toluene; (B) a droplet tilted at an angle to the field direction before twisting and then breaking up (C).

viscosity increased quickly during solvent evaporation, some of these long columns were frozen in before they broke up in the later stages of the solvent evaporation (see Figure 4B).

Parts A and C of Figure 11 show an additional phenomenon that was often observed. Some droplets that are elongated parallel to the electric field direction can be seen; these are most probably inside the phases that have been elongated perpendicular to the field direction. Thus, these are probably droplets of the PVA that are trapped inside these distorted PS-rich phases.

Droplet Deformation: Comparison with Theory. All our experimental observations indicated that when the dispersed phase (PVA-rich or PMMA-rich) had a higher dielectric constant and conductivity than the matrix phase (PS-rich) in the PS/PVA/toluene and PS/PMMA/toluene systems, the elongation of the dispersed phase was in the field direction. On the other hand, when the dispersed phase (PS-rich) had a smaller dielectric constant and conductivity than the matrix (PVA-rich or PMMA-rich), the droplet elongation was perpendicular to the field direction. As mentioned in the Introduction, the pure dielectric theory[21] predicts the existence of elongation parallel to the field direction only, no matter whether the droplet has a higher or smaller dielectric constant than the matrix. Thus, it is only a leaky dielectric theory like that of Torza et al.[22] that can predict the existence of deformations both parallel and perpendicular to the field direction. This theory leads to a discrimination function, Φ, given by

$$\Phi = S(R^2 + 1) - 2 + 3(SR - 1)(2M + 3)/(5M + 5) \quad (1)$$

where

$$S = \frac{\epsilon_m}{\epsilon_d}, \qquad R = \frac{\sigma_d}{\sigma_m}, \qquad M = \frac{\eta_m}{\eta_d} \quad (2)$$

and ϵ_m and ϵ_d, σ_m and σ_d, and η_m and η_d are the dielectric constants, conductivities, and viscosities of the matrix and the droplet, respectively. The direction of the deformation is given by the sign of Φ:

$\Phi > 0$ (elongation parallel to the field direction, prolate ellipsoid formed)

$\Phi = 0$ (no droplet deformation)

$\Phi < 0$ (elongation perpendicular to the field direction, oblate ellipsoid formed)

On the basis of the data in Tables 2 and 3, we obtain $\Phi > 0$ when the dispersed phase is the PVA- or PMMA-rich phase and the matrix is the coexisting PS-rich phase and $\Phi < 0$ when the dispersed phase is the PS-rich phase and the matrix is the coexisting PVA- or PMMA-rich phase.

Therefore, the Torza et al.[22] theory predicts that the droplet elongation should be in the field direction if the PVA- or PMMA-rich phase is the dispersed phase or perpendicular to the field direction if the PS-rich phase is the dispersed phase. This is in agreement with our observations in the PS/PVA/toluene and PS/PMMA/toluene mixtures. The key element in this theory is the conductivity effect which introduces free charges on the droplet/matrix interfaces, leading to tangential stresses at the interfaces. The tangential stresses, in turn, induce flow both inside and outside the droplets. These cause electrohydrodynamic normal stresses at the droplet interfaces in addition to the usual purely electrical stresses. Thus, the discrimination function Φ contains both purely electrical (the first two terms on the right-hand side of eq 1) and electrohydrodynamic (the third term on the right-hand side of eq 1) contributions to droplet deformation. The sign of the induced free charge depends on the product of the conductivity ratio, R, and the dielectric constant ratio, S. Figure 12 shows a schematic representation of the free charge distribution and the direction of fluid flow under a uniform dc electric field. When $SR = 1$, there is no free charge on the droplet/matrix interface. Although the Torza et al. theory[22] successfully predicted the direction of droplet deformation in our polymer systems, it was not adequate to analyze the magnitude of the deformation since, as explicitly stated by the authors, it is only suitable for small deformations and cannot predict droplet breakup as observed in our experiments.

The importance of the conductivity ratio in droplet deformation can also be seen by comparing the magnitude of the deformations in the PS/PVA/toluene and PS/PMMA/toluene mixtures. As seen in Table 2, the dielectric constant ratios S (PVA-rich vs PS-rich phase) in the PS/PVA/toluene mixtures were similar to those (PMMA-rich vs PS-rich phase) in the PS/PMMA/toluene mixtures, between 1.1 and 1.7. The interfacial tensions, as shown in Table 3, in the PS/PMMA/toluene system were smaller than those in the PS/PVA/toluene system at the same solvent content. Therefore, if the conductivity effect is neglected, the droplet deformations in the PS/PMMA/toluene mixtures should be comparable to (or even larger than) those in the PS/PVA/toluene mixtures using the pure dielectric theory.[21] However, we ob-

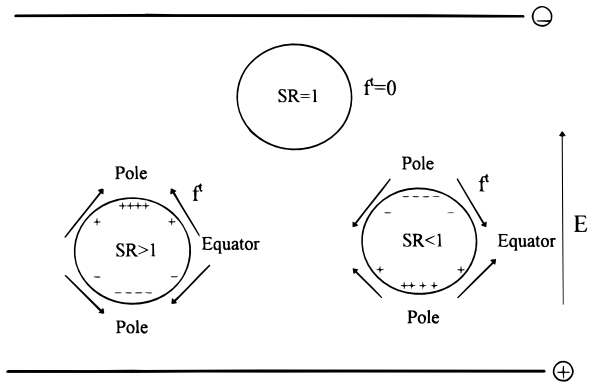

Figure 12. Instantaneous free charge distribution and the direction of the electric tangential stress f^t at the interface in an electric field. When $SR < 1$, the hemisphere facing the negative electrode becomes negatively charged, with f^t inducing a pole-to-equator fluid flow; the reverse occurs when $SR > 1$, with f^t inducing an equator-to-pole fluid flow.

served that the deformations in the PS/PVA/toluene mixtures were much larger than those in the PS/PMMA/toluene mixtures (comparing Figures 4 and 7). This is due to the fact that the conductivity ratios (dividing the larger conductivity by the smaller one) between the two coexisting phases in the PS/PVA/toluene mixtures were much larger than that in the PS/PMMA/toluene mixtures, especially at high polymer concentrations. This conclusion is supported by the observation that deformations in PS/PMMA/toluene mixtures increased dramatically with increasing conductivity difference when lithium triflate was added to one of the PS/PMMA/toluene mixtures to selectively enhance the conductivity of the PMMA-rich phase. As seen in Table 2, the conductivity ratio (PMMA-rich vs PS-rich) increased from 5.4 to 41 upon the addition of LiT (at 20% polymer content), while the dielectric constant ratio changed little.

Pearl Chain Formation: Comparison with Theory. Pearl chain formation in our system is a process of mutual dielectrophoresis,[34] as is also seen in electrorheological (ER) fluids.[35] Dielectrophoresis refers to the translational motion of polarizable neutral particles in a nonuniform electric field. The central feature of pearl chain formation is the mutual attraction between the particles or droplets due to the induced polarization in an electric field. For a spherical particle or droplet, the induced dipole moment can be written as[35]

$$p = \beta r_0^3 E \tag{3}$$

where p is the induced dipole moment, r_0 is the radius of the droplet, E is the applied field, and β is the effective polarizability.

The origin of the polarization in an ER fluid, however, is still in debate and has been recently reviewed by Zukoski.[36] Basically, two kinds of polarization can be considered, namely, electrostatic and interfacial polarization. Considering the electrostatic polarization, both the droplets and the medium are assumed to be perfectly insulting dielectrics and the effective polarizability β is determined only by the dielectric constant ratio:[36]

$$\beta = \frac{\epsilon_d - \epsilon_m}{\epsilon_d + 2\epsilon_m} = \frac{\epsilon_d/\epsilon_m - 1}{\epsilon_d/\epsilon_m + 2} \tag{4}$$

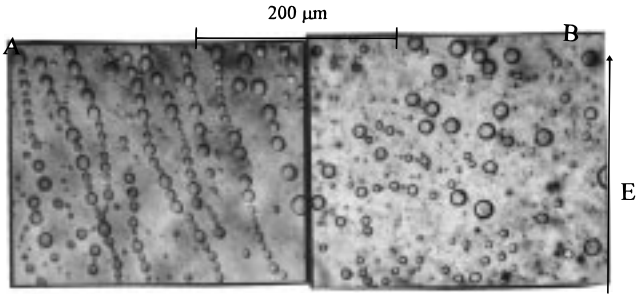

Figure 13. Effect of frequency of the applied field on pearl chains in a blend of 9/1 (w/w) PS/PVA in toluene (A) at E = 3.3 kV/cm and $\nu = 0$ Hz and (B) the field switched to $\nu = 60$ Hz and $E = 6.6$ kV/cm.

When considering the interfacial polarization, the conductivity effect (thus, the free charge accumulation at the droplet interface) is taken into account and β is given by[36]

$$\beta^* = \frac{\sigma_d^* - \sigma_m^*}{\sigma_d^* + 2\sigma_m^*} = \frac{\sigma_d^*/\sigma_m^* - 1}{\sigma_d^*/\sigma_m^* + 2} \tag{5}$$

where σ_d^* and σ_m^* are the complex conductivities of the dispersed phase and the medium, respectively, and are given by

$$\sigma_d^* = \sigma_d + i\omega\epsilon_0\epsilon_d \tag{6}$$

$$\sigma_m^* = \sigma_m + i\omega\epsilon_0\epsilon_m \tag{7}$$

where ω is the angular frequency of the applied field and σ_d and σ_m are the conductivities of the dispersed phase and the medium, respectively.

On the basis of eqs 5−7, one has

$$\lim_{\omega\to 0} \beta^+ = \frac{\sigma_d - \sigma_m}{\sigma_d + 2\sigma_m} \tag{8}$$

$$\lim_{\omega\to \infty} \beta^+ = \frac{\epsilon_d - \epsilon_m}{\epsilon_d + 2\epsilon_m} \tag{9}$$

From eqs 8 and 9, one can see that (i) at the low-frequency limit ($\omega \to 0$), the free charge effect is dominant and the polarization is determined only by the conductivity ratio, and (ii) at the high-frequency limit ($\omega \to \infty$), the free charge effect disappears and the polarization is determined only by the dielectric constant ratio. The crossover or characteristic frequency, f_c, for the transition from interfacial polarization (with the free charge effect) to electrostatic polarization (without the free charge effect) is given by

$$f_c = \frac{\omega_c}{2\pi} = \frac{\sigma_d + 2\sigma_m}{\epsilon_0(\epsilon_d + 2\epsilon_m)} \tag{10}$$

For droplets of the PVA-rich phase dispersed in the PS-rich matrix at 20 wt % total polymer, the calculated characteristic frequency, f_c, using the data in Table 2 and eq 10 is 2.7 Hz. In the experiments, it was observed that pearl chains formed easily in this blend in a dc field (Figure 13A); however, no pearl chains were observed in the same blend when the applied frequency was >2 Hz, for example, at $f = 60$ Hz as shown in Figure 13B.

The importance of the conductivity effect in pearl chain formation was also observed in experiments on

PS/PMMA/toluene mixtures in the presence and absence of LiT salt. As mentioned above, no pearl chain formation was observed in the PS/PMMA/toluene system in the absence of LiT in a dc field, probably due to a relatively low conductivity ratio between the two phases. After adding LiT salt to the PS/PMMA mixtures, pearl chains were observed. The conductivity ratio increased dramatically upon the addition of LiT, while the dielectric constant ratio remained about the same (see Table 2). Thus, it appears that the formation of pearl chains in the presence of LiT in the PS/PMMA/toluene mixtures is determined mostly by the conductivity ratio between the phases, at least in a dc field.

Stability of Column Structures in a dc Electric Field. Long columns were fairly stable in a dc field during solvent evaporation (Figures 4A and 5B). On the other hand, if the electric field was turned off while sufficient solvent was present, every column broke up into a number of small spheres. This result is consistent with the observations of Venugopal et al.[4] This shows that the electric field stabilizes the columns. The breakup of a long column under a zero external field is due to the Rayleigh or capillary instability.[37] Rayleigh showed that any small disturbance in the column curvature will grow provided the wavelength of the disturbance exceeds the circumference of the column. As a result, the column eventually breaks up into several small droplets instead of retracting to one large one. A later theoretical study[38] showed that the Rayleigh instability decreases a great deal and columns become much more stable under the influence of a hydrodynamic field. This is consistent with some experimental work by Taylor.[39] According to Tomotika,[40] the growth of the disturbance in the Rayleigh instability is proportional to the interfacial tension and inversely proportional to the viscosity of the medium and the radius of the column. This means that the thinner the column, the greater the instability. Some columns broke up in the electric field, but very often the breakup involved only part of a column (see Figure 4A). This shows that the Rayleigh instability was suppressed by the electric field, probably because of a competition between the electric force, which tries to preserve the columnar deformation, and the Rayleigh instability, which tries to break up the column. If enough solvent was present to preserve the fluidity of the system, breakup of all the columns occurred as the electric field was reduced, but before the electric field became zero. We have not been able to find any theoretical work on the effect of an electric field on the Rayleigh instability.

Morphology Development in a dc Field during Solvent Evaporation. Stable structures were only formed in the late stages of solvent evaporation, so that the final morphology obtained was not determined by the properties shown in Tables 2 and 3. During the course of phase separation with continuous removal of solvent, the equilibrium compositions expected from phase diagrams such as Figures 2 and 3 are probably never reached, because of the low diffusivities of the polymers in concentrated solutions. An experiment was done in which the deformation of a PMMA-rich droplet obtained using method 2 (coexisting phases prepared as such) was compared with the deformation of a second PMMA-rich droplet of equal size that was obtained using method 1 (solvent evaporation from a single-phase solution), in a comparable electric field. The mass of the solution from method 1 was measured at various times during the solvent evaporation until the total polymer concentration and composition of this solution was the same as that obtained using method 2. At this point, the system was searched for a droplet of the correct size for comparison with one of the droplets observed using method 2. The deformations of the PMMA-rich droplets suspended in the PS-rich matrix were generally larger during the solvent evaporation (method 1) than the deformation from the coexisting phase injection experiment (method 2) at the same solvent content. In a particular comparison, a droplet observed during solvent evaporation had an axial ratio of 2.7 at $E = 1.6$ kV/cm, while a droplet prepared using method 2 had an axial ratio of 1.5 at $E = 2.3$ kV/cm, a higher electric field. This larger droplet deformation during solvent evaporation is probably due to nonequilibrium phase separation in the course of the evaporation, that is, the phases cannot achieve their equilibrium (polymer/polymer) composition but will retain a composition closer to that which was the equilibrium composition at higher solvent composition. The nonequilibrium phases probably retain the smaller interfacial tensions of the more solvent-rich phases, leading to larger deformations during solvent evaporation. This nonequilibrium phase separation also implies that the other phase properties (dielectric constants and conductivities) of the dispersed phase and the matrix during solvent evaporation are different from those of the corresponding coexisting phases. The degree of the nonequilibrium phase separation in our systems is difficult to estimate.

Figures 4, 5, and 7 show that the droplet deformations observed in the PS/PVA/toluene system were generally much larger than those observed in the PS/PMMA/toluene system. This can be attributed to the much greater conductivity ratio (if the higher conductivity is divided by the lower) in the former system. One may note, in Figure 5A, that some droplets of the PVA-rich phase in the PS-rich matrix had pointed ends. Such a pointed shape was not predicted by the Torza et al.[22] theory since an ellipsoidal shape is assumed in the derivations. However, in a numerical study of a (leaky dielectric) droplet deformed in the electric field direction, Sherwood[41] showed that, in the case of a leaky dielectric, the pointed ends are the result of a high conductivity ratio, which leads to very large normal stresses at the droplet ends. Also, Garton and Krasucki[21] showed experimental data on a conducting water droplet which had pointed ends in a hydrocarbon oil just as small droplets were being ejected while the system was in a dc electric field. This system, too, can be viewed using the leaky dielectric theory with a high conductivity ratio between the water and the oil. Therefore, the observed pointed ends of some of the PVA-rich droplets in the PS/PVA/toluene mixtures can be viewed as another result of the high conductivity ratio during solvent evaporation. It is interesting to note (Figure 14) that an occasional PMMA-rich phase, injected into a PS-rich phase, exhibited the ejection of small droplets from at least one pointed end on some occasions.

In the case of the PS/PMMA/toluene system, droplet deformation was relatively large (not shown) in the early stages of phase separation, probably due to the small interfacial tensions. In the late stages of the evaporation, the deformation became small even at relatively large fields. The final morphology usually contained distorted droplets randomly distributed in the matrix

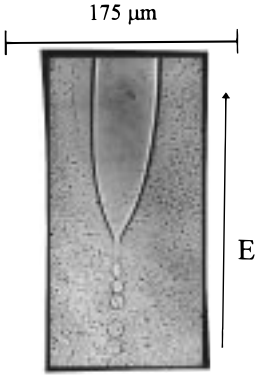

Figure 14. Small droplet ejection from one end of a PMMA-rich large droplet which had been injected into the PS-rich phase at $E = 1$ kV/cm. The coexisting phases were from a 1/1/8 PS/PMMA/toluene mixture.

with deformation either parallel (if the PMMA-rich phase was the dispersed phase) or perpendicular (if PS-rich phase was the dispersed phase) to the field direction. The conductivity ratios (dividing the larger value by the smaller) of the coexisting phases were smaller than those in PS/PVA/toluene mixtures, especially at relatively high polymer concentrations. This indicates that the ability of PMMA to associate with ionic species (although greater than PS) was much lower than that of PVA.

In the case of the PS/PB/toluene mixtures, all final phase deformations were very small even at a very large electric field as shown in Figure 8. This is almost certainly because the conductivities of the PB-rich and PS-rich phases were almost the same due to the very close dielectric constants of PS and PB. This result is somewhat different from the observation of no phase distortions at all in this system by Venugopal et al.;[4] our polymers were not exactly the same as those examined in the previous work, and the ion content may well have been different. As seen in Figure 8, some PS-rich droplets deformed slightly parallel to the field direction, some deformed slightly perpendicular to the field direction, and some appeared to show no deformation at all. For PS-rich droplets dispersed in the matrix of the PB-rich phase, the calculated value of the discrimination function, Φ, is -0.18, based on the data in Table 2 and eq 1. This means that the PS-rich droplets should elongate perpendicular to the field direction. Therefore, the observation of some elongations parallel to the field direction and some undeformed droplets suggests that the phase properties in the electric field were not necessarily the same as those measured in the absence of a field; there may have been a change in the conductivity ratio of some of the droplets, those deformed parallel to the field direction or not at all. Since the conductivity ratio was very close to 1, fluctuations in ion concentrations, thus also conductivities, of the PS-rich and PB-rich phases may have become important, especially in a large electric field in which one has ion migration and fluid motion. As a result, some PS-rich droplets may have become a little less conducting than the PB matrix, and some may have achieved the same conductivity as the PB matrix, leading to the observations shown in Figure 8. Similar observations were made by injecting PS-rich droplets into a PB-rich matrix from the coexisting phases (see Figure 9).

Conclusions

1. When a dc electric field is applied to a single-phase solution containing two immiscible homopolymers in a mutual solvent during solvent evaporation, the droplets of the dispersed phases can be deformed into ellipsoids with their major axes either parallel or perpendicular to the field direction; these can form pearl chains in the field direction, or they can form columns either parallel or perpendicular to the field direction. Electric-field-induced breakup of droplets and columns can also take place during solvent evaporation.

2. It was found that the conductivity ratio between the droplet and the matrix phases was extremely important in determining both the direction and the magnitude of droplet deformation in a dc field in the ternary polymer mixtures under study, even though the absolute values of the conductivities of the mixtures were extremely low. Pearl chain formation in these systems in a dc field was determined mostly by the conductivity ratio.

Acknowledgment. This paper is based upon work partly supported by the National Science Foundation under Grant DMR-9202988. Many thanks go to the Anton Paar Co. for a partial subsidy for the purchase of the densitometer used in this work. The authors acknowledge Gary E. Wnek for many fruitful discussions and also for the use of the dielectric constant and conductivity apparatus in his laboratory. Many thanks also go to Joseph Serpico for help in instrument operation.

References and Notes

(1) Present address: Plastics Division, General Electric Co., 1 Lexan Lane, Mt. Vernon, IN 47620.
(2) Moriya, S.; Adachi, K.; Kotaka, T. *Polym. Commun.* **1985**, *23*, 235.
(3) Venugopal, G.; Krause, S.; Wnek, G. E. *J. Polym. Sci., Part C: Polym. Lett.* **1989**, *27*, 497.
(4) Venugopal, G.; Krause, S. *Macromolecules* **1992**, *25*, 4626.
(5) Venugopal, F.; Krause, S.; Wnek, G. E. *Chem. Mater.* **1992**, *4*, 1334.
(6) Serpico, J. M.; Wnek, G. E.; Krause, S.; Smith, T. W.; Luca, D. J.; Van Laeken, A. *Macromolecules* **1991**, *24*, 6879.
(7) Sterzynski, T.; Garbarczyk, J. *J. Mater. Sci.* **1991**, *26*, 6357.
(8) Shiga, T.; Okada, A.; Karauchi, T. *Macromolecules* **1993**, *26*, 6958.
(9) Winoto, D.; Carr, S. H. *Macromolecules* **1996**, *29*, 5149.
(10) Wirtz, D.; Berend, K.; Fuller, G. G. *Macromolecules* **1992**, *25*, 7234.
(11) Wirtz, D.; Fuller, G. G. *Phys. Rev. Let.* **1993**, *71*, 2236.
(12) Moriya, S.; Adachi, K.; Kotaka, K. *Langmuir* **1986**, *2*, 155.
(13) Moriya, S.; Adachi, K.; Kotaka, K. *Langmuir* **1986**, *2*, 161.
(14) Amundson, K.; Helfand, E.; Davis, D. D.; Quan, X.; Patel, S. S.; Smith, S. D. *Macromolecules* **1991**, *24*, 6546.
(15) Amundson, K.; Helfand, E.; Quan, X.; Smith, S. D. *Macromolecules* **1993**, *26*, 2698.
(16) Amundson, K.; Helfand, E.; Quan, X.; Hudson, S. D.; Smith, S. D. *Macromolecules* **1994**, *27*, 6559.
(17) Morkved, T. L.; Lu, M.; Urbas, A. M.; Ehrichs, E. E.; Jaeger, H. M.; Mansky, P.; Russell, T. P. *Science* **1996**, *273*, 931.
(18) Serpico, J. M.; Wnek, G. E.; Krause, S.; Smith, T. W.; Luca, D. J.; Van Laeken, A. *Macromolecules* **1992**, *25*, 6373.
(19) Randall, C. A.; Miller, D.; Adair, J.; Bhalla, A. *J. Mater. Res.* **1993**, *8*, 899.
(20) Bowen, C. P.; Bhalla, A. S.; Newnham, R. E.; Randall, C. A. *J. Mater. Res.* **1994**, *9*, 781.
(21) Garton, C. G.; Krasucki, Z. *Proc. R. Soc. London* **1964**, *A280*, 211.
(22) Torza, S.; Rox, R. G.; Mason, S. G. *Philos. Trans. R. Soc. London* **1971**, *269*, 295.
(23) Venugopal, G.; Krause, S.; Wnek, G. E. *Polymer* **1993**, *34*, 3241.

(24) Trent, J. S.; Scheinbeim, J. I.; Couchman, P. R. *J. Polym. Sci., Polym. Lett. Ed.* **1981**, *19*, 315.
(25) Heinrich, M.; Wolf, B. A. *Polymer* **1992**, *33*, 1926.
(26) Kurata, M. *Thermodynamics of Polymer Solutions*; Harwood Academic: New York, 1982.
(27) Kamide, K. *Thermodynamics of Polymer Solutions. Phase Equilibria and Critical Phenomena*; Elsevier: New York, 1990.
(28) Tompa, H. *Polymer Solutions*; Butterworth: London, 1956.
(29) Barton, A. F. M. *Handbook of Polymer−Liquid Interaction Parameters and Solubility Parameters*; CRC Press: Boca Raton, FL, 1990.
(30) Brandrup, J., Immergut, E. H., Eds. *Polymer Handbook*, 3rd ed.; Wiley-Interscience: New York, 1989.
(31) Weast, R. C., Ed. *CRC Handbook of Chemistry and Physics*, 56th ed.; CRC Press: Cleveland, OH, 1988.
(32) Adamczewski, I. *Ionization, Conductivity and Breakdown in Dielectric Liquids*; Barnes & Noble: New York, 1969.
(33) Venugopal, G. Ph.D. Thesis, Rensselaer Polytechnic Institute, Troy, NY, 1991.
(34) Pohl, H. A. *Dielectrophoresis, the behavior of neutral matter in nonuniform electric fields*; Cambridge University Press: New York, 1978.
(35) Halsey, T. C. *Science* **1992**, *258*, 761.
(36) Zukoski, C. F. *Annu. Rev. Mater. Sci.* **1993**, *23*, 45.
(37) (a) Rayleigh, Lord. *Proc. London Math. Soc.* **1879**, *10*, 4. (b) Rayleigh, Lord. *Proc. R. Soc. London* **1879**, *29*, 71.
(38) Tomotika, S. *Proc. R. Soc. London* **1936**, *A153*, 302.
(39) Taylor, G. I. *Proc. R. Soc. London* **1934**, *A146*, 501.
(40) Tomotika, S. *Proc. R. Soc. London* **1935**, *A150*, 322.
(41) Sherwood, J. D. *J. Fluid Mech.* **1988**, *188*, 133.

MA971650Z